

## Supporting Information

# Photochromic Paper Indicators for Acidic Food Spoilage Detection

*Maria E. Genovese,<sup>\*,†</sup> Sinoj Abraham,<sup>§</sup> Gianvito Caputo,<sup>‡</sup> Gabriele Nanni,<sup>†</sup> Surjith K. Kumaran,<sup>§</sup>  
Carlo D. Montemagno,<sup>¶</sup> Athanassia Athanassiou<sup>†</sup> and Despina Fragouli<sup>\*,†</sup>*

<sup>†</sup>Smart Materials, Istituto Italiano di Tecnologia, Via Morego 30, 16163, Genova, Italy

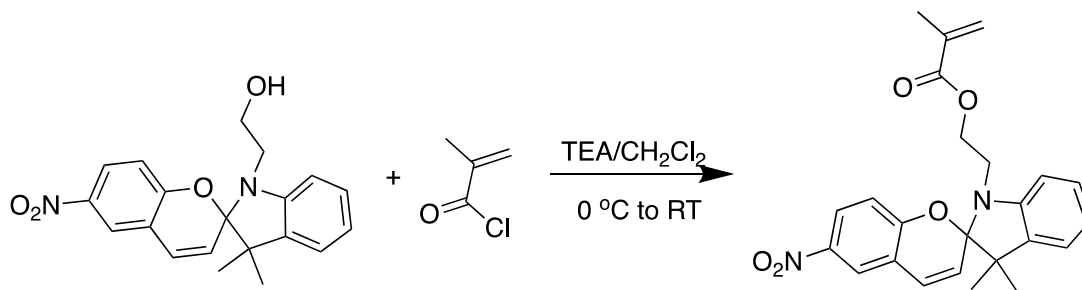
<sup>§</sup>Department of Chemical and Materials Engineering, University of Alberta, 9211-116 Street  
NW, Edmonton, T6G 1H9, Canada

<sup>¶</sup>Southern Illinois University, 1230 Lincoln Drive, Carbondale IL, 62901, USA

<sup>‡</sup>*Current address: Nanochemistry, Istituto Italiano di Tecnologia, Via Morego 30, 16163,  
Genova, Italy*

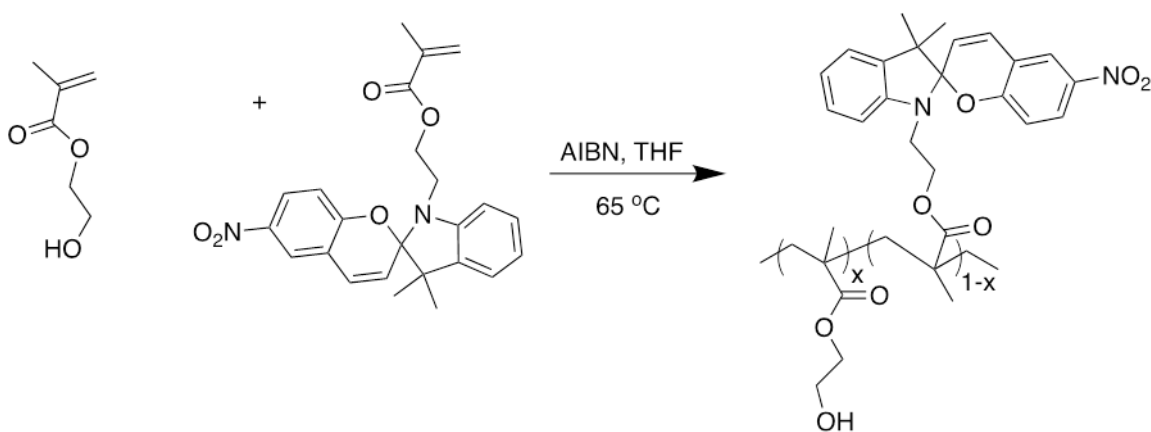
KEYWORDS cellulose, photochromism, spiropyrans, indicators, optical detection, food  
spoilage.

### SPMA Synthesis



**Scheme S1.** Synthetic scheme for the preparation of Spiropyran methacrylate monomer (SPMA).

### SP-PHEMA Synthesis



**Scheme S2.** Synthetic scheme for the preparation of Poly(2-Hydroxyethyl methacrylate-co-Spiropyran methacrylate) (SP-PHEMA).

## SP-PHEMA Characterization

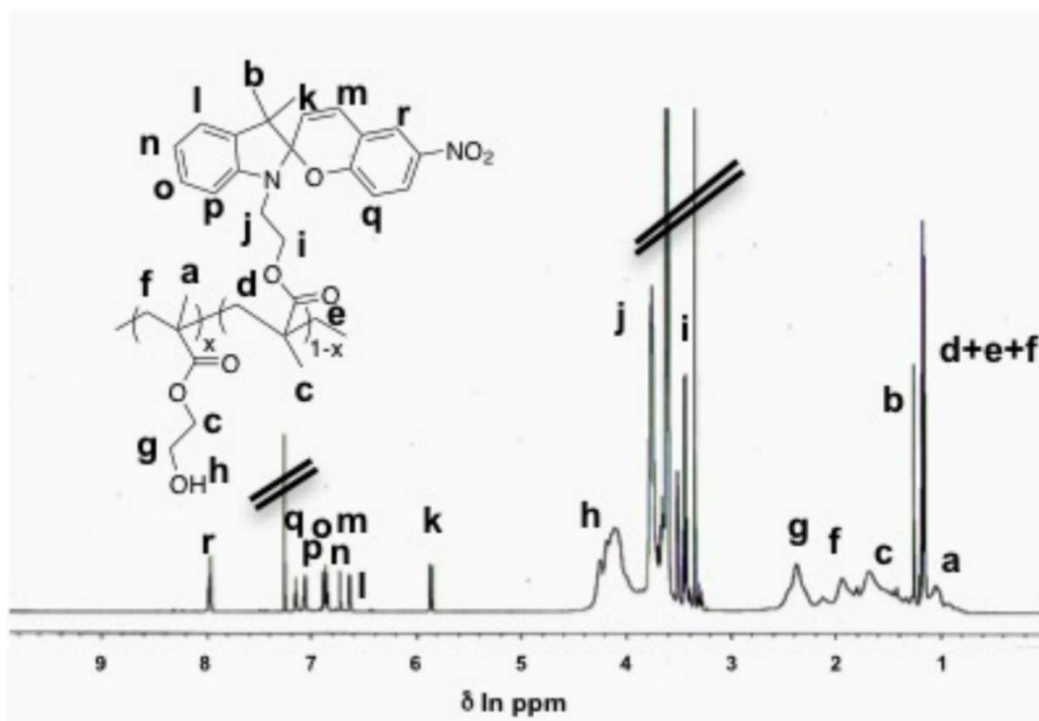


**Figure S1.**  $^1\text{H}$  NMR spectrum of Poly(2-Hydroxyethyl methacrylate-co-Spiropyran methacrylate) in  $\text{CDCl}_3$ .

## Chemical characterization of FP/SP-PHEMA

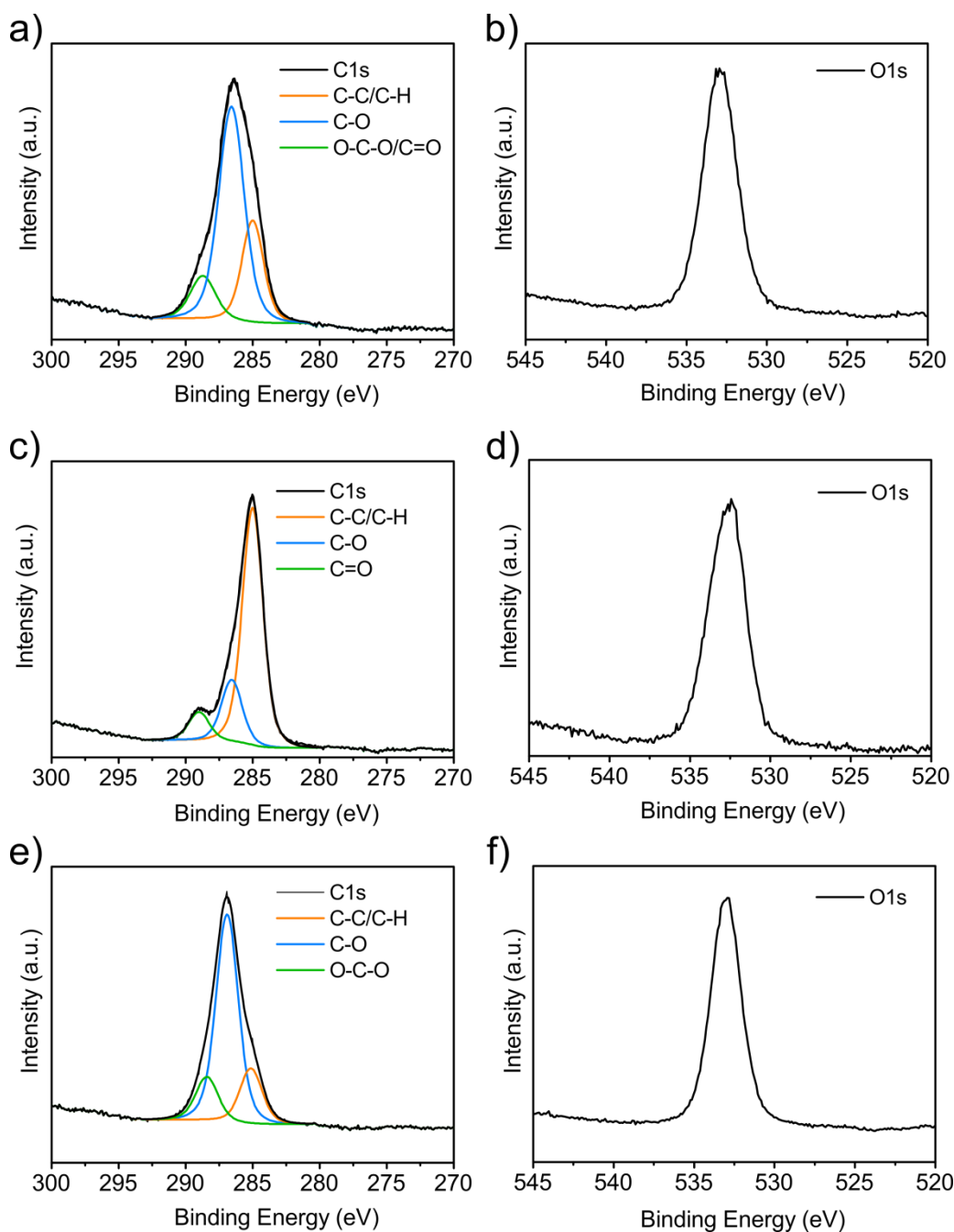


**Figure S2.** High resolution C1s and O1s XPS spectra of FP/SP-PHEMA a) and b), SP-PHEMA c) and d) and untreated FP e) and f). The C1s components obtained by deconvolution are also indicated.

As shown in Figure S2, although the high resolution O1s spectrum of FP/SP-PHEMA did not significantly differ from that of the untreated FP, the binding energy (BE) of C1s (286.4 eV)

exhibited an intermediate value between the BEs of FP (286.9 eV) and of SP-PHEMA (285.0 eV) (Table S1), revealing a possible interaction between the SP-PHEMA and the cellulose. More specifically, from the deconvolution of the C1s peak of FP/SP-PHEMA, an increase of 7% in the C-C/C-H component was registered, consistently with the incorporation of the aliphatic polymer chains in the material, and, in parallel, a shift of -0.3 eV in the C-O component (286.6 eV) was observed with respect to the untreated FP (286.9 eV), matching the value determined for SP-PHEMA (Table S2). On top of that, the variation of +0.3eV and -0.3 eV in the BE of the O-C-O/C=O components of FP/SP-PHEMA (288.7eV) with respect to the BE of O-C-O of untreated FP (288.4eV) and to the BE of C=O of SP-PHEMA (289.0eV) (Table S2) confirms a modification in the chemical environment possibly ascribed to interactions *via* hydrogen bonding between the hydroxyl groups of cellulose and the ester groups of the acrylic polymer, similarly to what reported for composites of cellulose with polyesters.<sup>1</sup>

**Table S1.** C1s and O1s BEs of FP, SP-PHEMA and FP/SP-PHEMA extracted from the XPS spectra.

Sample	C1s (eV)	O1s (eV)
FP	286.9±0.1	533.0±0.1
SP-PHEMA	285.0±0.1	532.5±0.1
FP/SP-PHEMA	286.4±0.1	533.0±0.1

**Table S2.** C1s BE components obtained by deconvolution and relative percentage for FP, SP-PHEMA and FP/SP PHEMA. Variations of  $\pm 0.1$  eV are in the range of the experimental error.

Sample	C-C/C-H (eV)	C-C/C-H (%)	C-O (eV)	C-O (%)	O-C-O/C=O (eV)	O-C-O/C=O (%)
FP	285.0 $\pm$ 0.1	18.1	286.9 $\pm$ 0.1	67.8	288.4 $\pm$ 0.1	14.1
SP-PHEMA	285.0 $\pm$ 0.1	72.5	286.6 $\pm$ 0.1	18.9	289.0 $\pm$ 0.1	8.6
FP/SP-PHEMA	285.0 $\pm$ 0.1	25.3	286.6 $\pm$ 0.1	62.4	288.7 $\pm$ 0.1	12.3

### Photochromic Properties

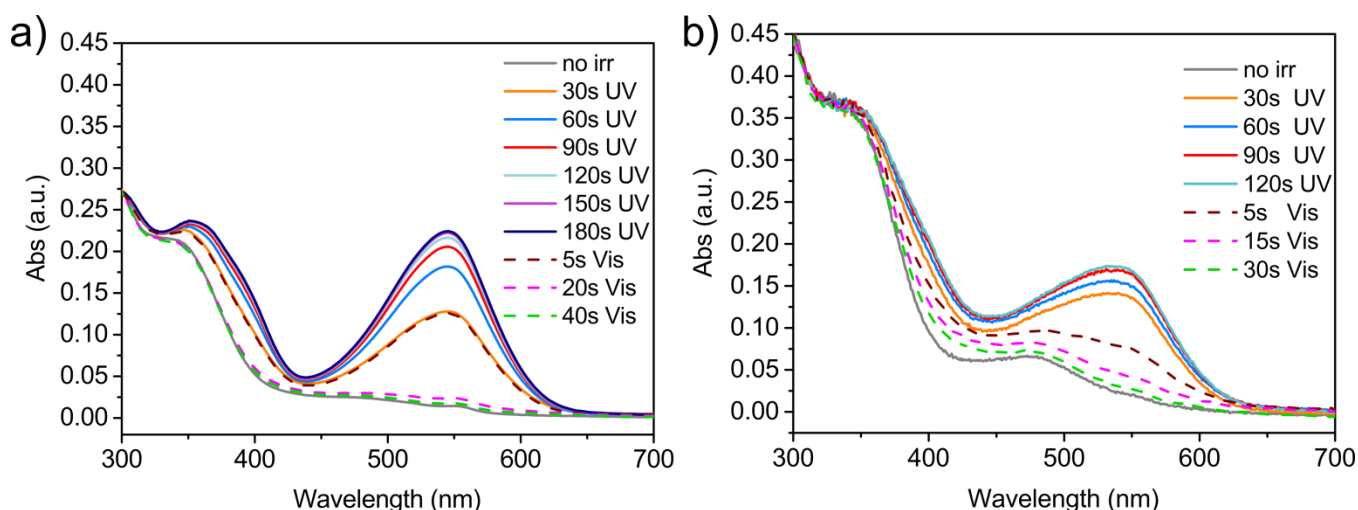


**Figure S3.** Absorption spectra of SP-PHEMA (a) and FP/SP-PHEMA (b) at different irradiation times with UV and Vis light.

As shown in Figure S4 and in Table S3, the spontaneous reversion of MC to SP in the dark was slower for the FP/SP-PHEMA composite compared to SP-PHEMA cast on glass, as 60 minutes after UV irradiation the absorbance of MC decreased to 87% and to 82% of its initial value in the glass coating and in the paper composite, respectively. The slower decay of the MC signal observed in FP/SP-PHEMA indicates an increased stability of the MC species upon incorporation in the paper network, which could be ascribed to the interactions of the zwitterionic molecules with the cellulose hydroxyl groups.<sup>2</sup>

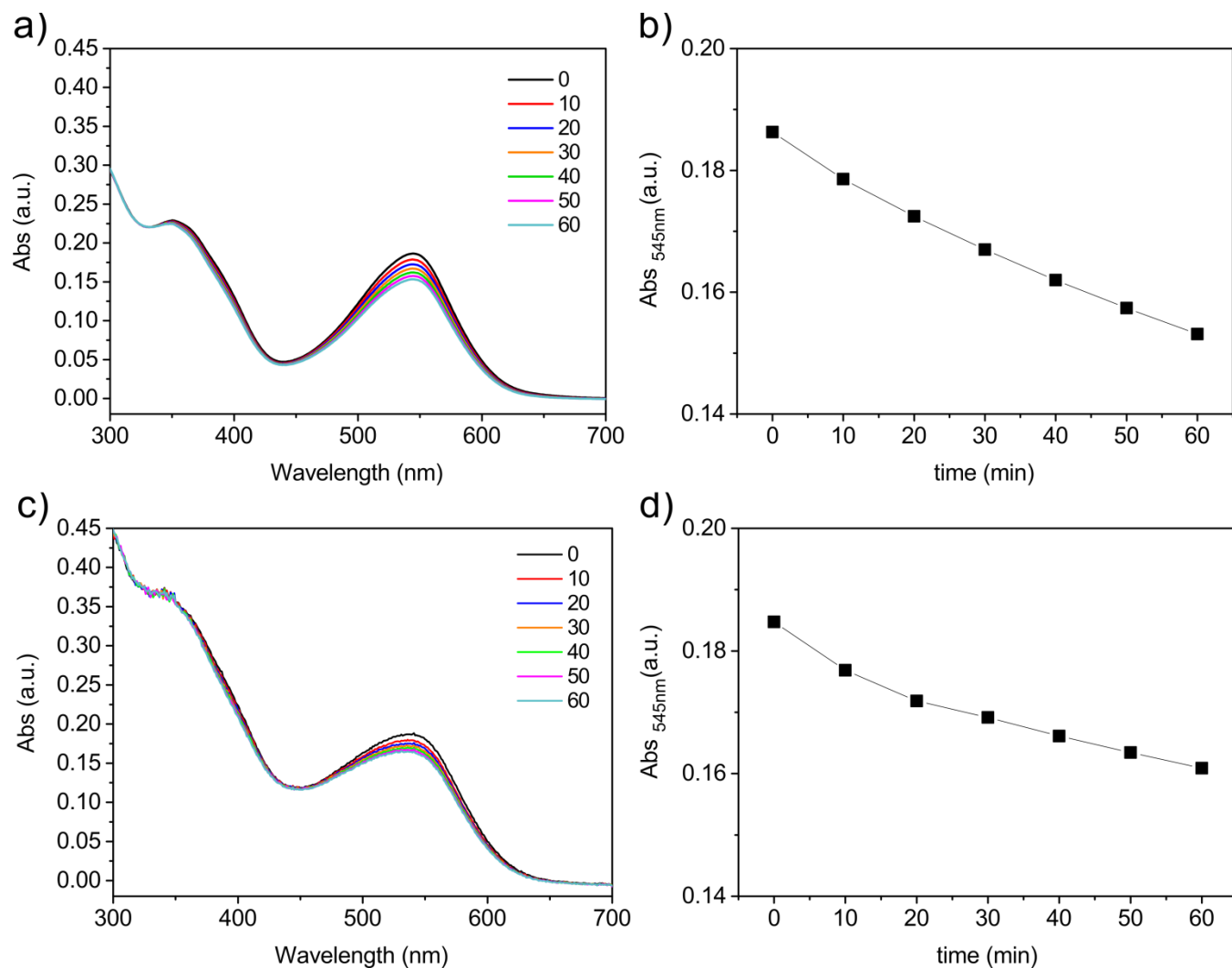


**Figure S4.** Absorption spectra and relative variation of the MC optical signal at 545 nm in SP-PHEMA deposited on glass (a) and (b) in FP/SP-PHEMA; (c,d) 0-60 minutes after UV irradiation and subsequent storage in the dark, respectively.

**Table S3.** Variation of the MC absorbance at 545 nm in SP-PHEMA and FF/SP-PHEMA samples stored in the dark for 0-60 minutes after UV irradiation.

Time (min)	Abs <sub>545 nm</sub> SP-PHEMA (%)	Abs <sub>545 nm</sub> FP/SP-PHEMA (%)
0	100.0	100.0
10	95.8	95.7
20	92.6	93.0
30	89.6	92.0
40	86.9	89.9
50	84.5	88.4
60	82.2	87.0



**Table S4.** Variation of the MC absorbance at 545 nm in SP-PHEMA and FF/SP-PHEMA samples upon alternate UV/Vis irradiation.

Cycle number	Abs <sub>545 nm</sub> SP-PHEMA (%)	Abs <sub>545 nm</sub> FP/SP-PHEMA (%)
1	100.0	100.0
10	90.8	100.0
20	81.0	93.5
30	69.4	86.7
40	57.0	79.9
50	38.0	70.3
60	21.2	67.4
70	-	65.2
80	-	61.9
90	-	57.0
100	-	54.1
110	-	52.2
120	-	49.0
130	-	41.0
140	-	24.8

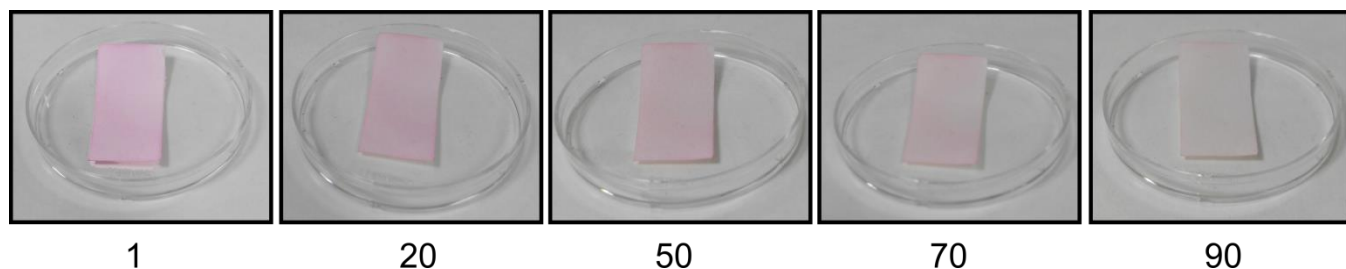
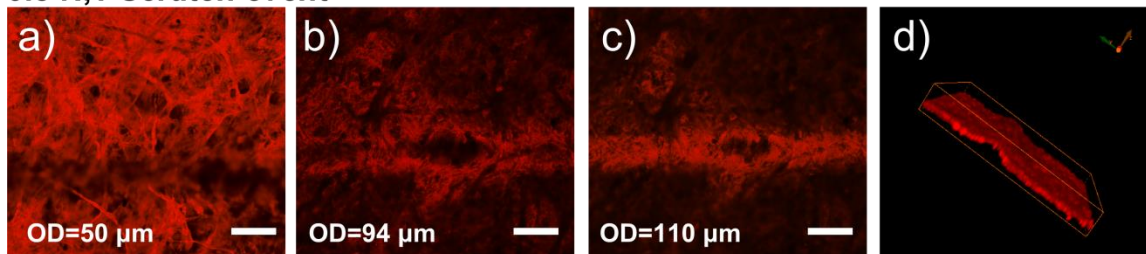


**Figure S5.** Photographs of a FF/SP-PHEMA sample after UV irradiation during 90 consecutive UV/Vis irradiation cycles. The cycle number is indicated for each photograph.

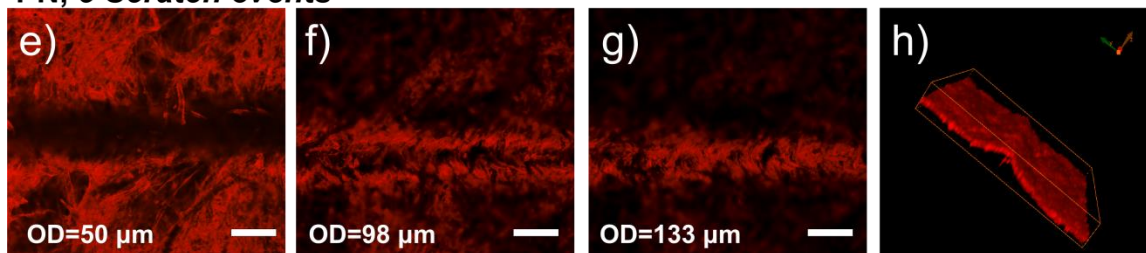
### **Durability**

In order to assess the durability of the SP-PHEMA coating on the FP, different areas of the FP/SP-PHEMA sample were scratched 1-10 times using different loads (0.5-2.0N) and then imaged through confocal microscopy after UV irradiation. As shown in Figure S6a, after the first scratch event with the lowest load (0.5 N), a thin darker area was visible on the surface, consistently with the removal of the material due to the scratching process. By increasing the load and the number of scratch events, the scratched dark area became larger and more evident (Figure S6 e, i). At the same time, the edges of the scratch progressively appeared more prominent and on different focal planes with respect to the surrounding area (Figure S6b,f and j), as the depth of the indented volume increased (Figure S6d,h and l). Interestingly, the fibrous features of the inner layers inside the scratch could still be detected in all samples, as revealed by the optical depths of the images (Figure S6c, g and k), indicating thus that the SP-PHEMA polymer is not confined on the superficial layers of the material but it penetrates deeply into the cellulose network. Such self-similarity ensures the replication of the materials functionalities, allowing to overcome the drawbacks of conventional coatings, in which the damage or removal of surface layers typically compromise their functional properties.

**0.5 N, 1 Scratch event**



**1 N, 5 Scratch events**



**2 N, 10 Scratch events**

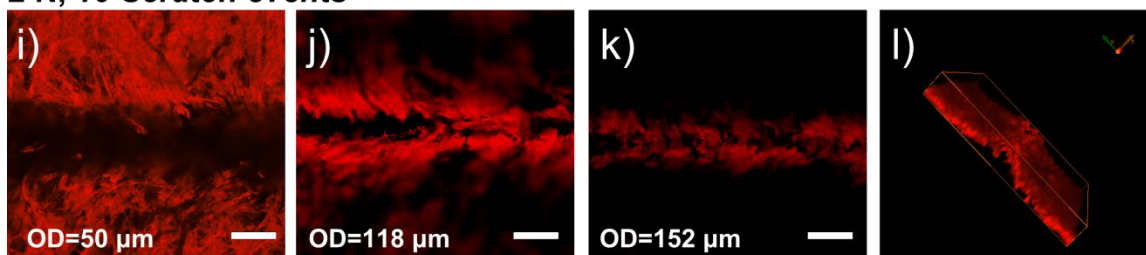


**Figure S6.** Confocal fluorescent images of UV irradiated FP/SP-PHEMA ( $\lambda_{\text{ex}} = 560 \text{ nm}$ ) after 1 scratch event at 0.5 N (a-d), after 5 scratch events at 1 N (e-h) and after 10 scratch events at 2 N (i-l). A zoom-in of the surfaces (a,e,i), scratch edges (b,f,j), and inner layers of the scratched areas (c,g,k) and the 3D- stack reconstruction of each scratch profile (d,h,l) are shown for each condition. The optical depth is reported for comparison in each image. The scale bar is 200  $\mu\text{m}$ . The 3D stacks have a size of 1272 x 1272  $\mu\text{m}^2$  and a thickness of 200  $\mu\text{m}$ .

## Acidic Food Spoilage Detection

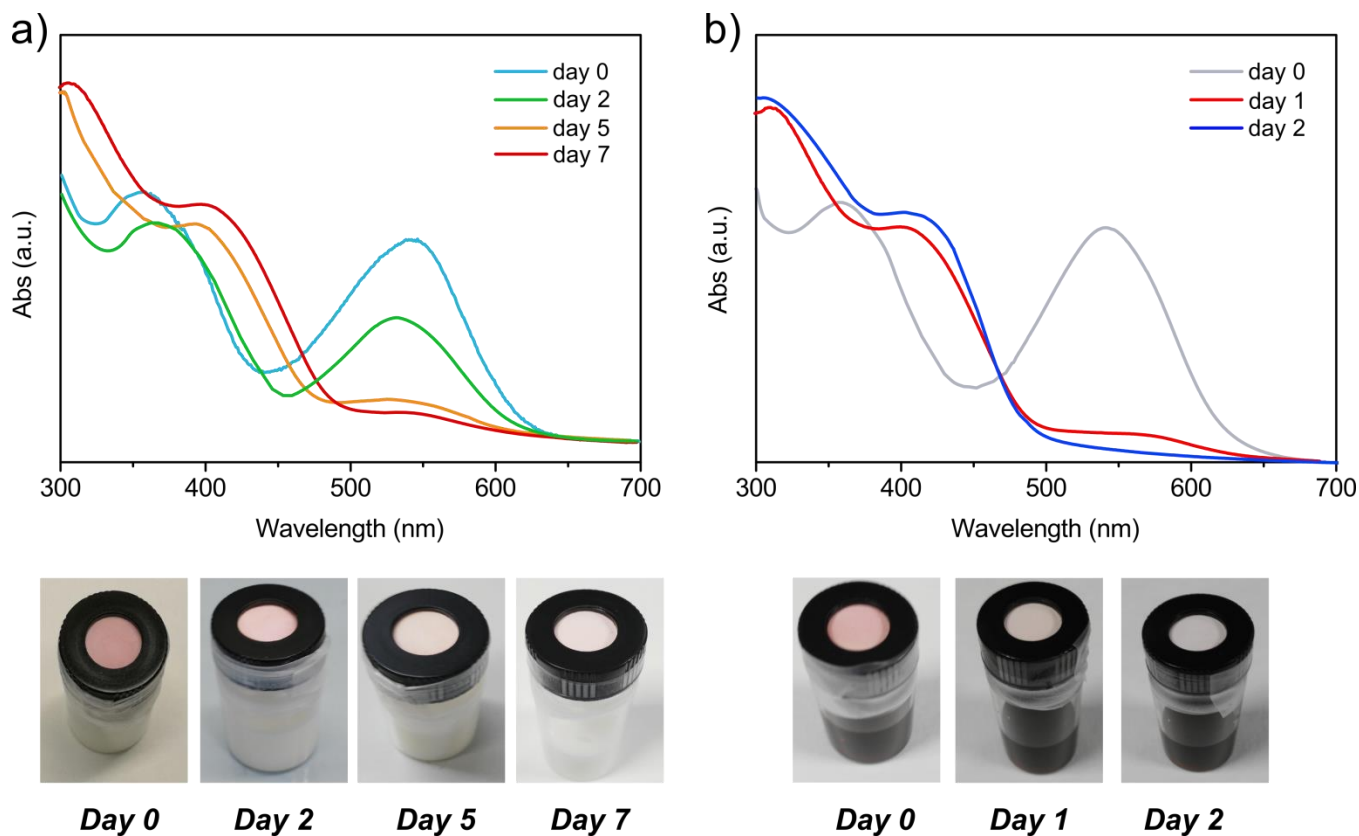


**Figure S7.** a) UV-Vis spectra of UV irradiated FF/SP-PHEMA caps used for UHT milk storage up to 7 days. b) UV-Vis spectra of UV irradiated FF/SP-PHEMA caps used for table red wine storage up to 2 days. Insets: Photos of the samples at the corresponding storage times. Similar spectral and color variations were observed with pasteurized milk and with the N and C types of red wine.

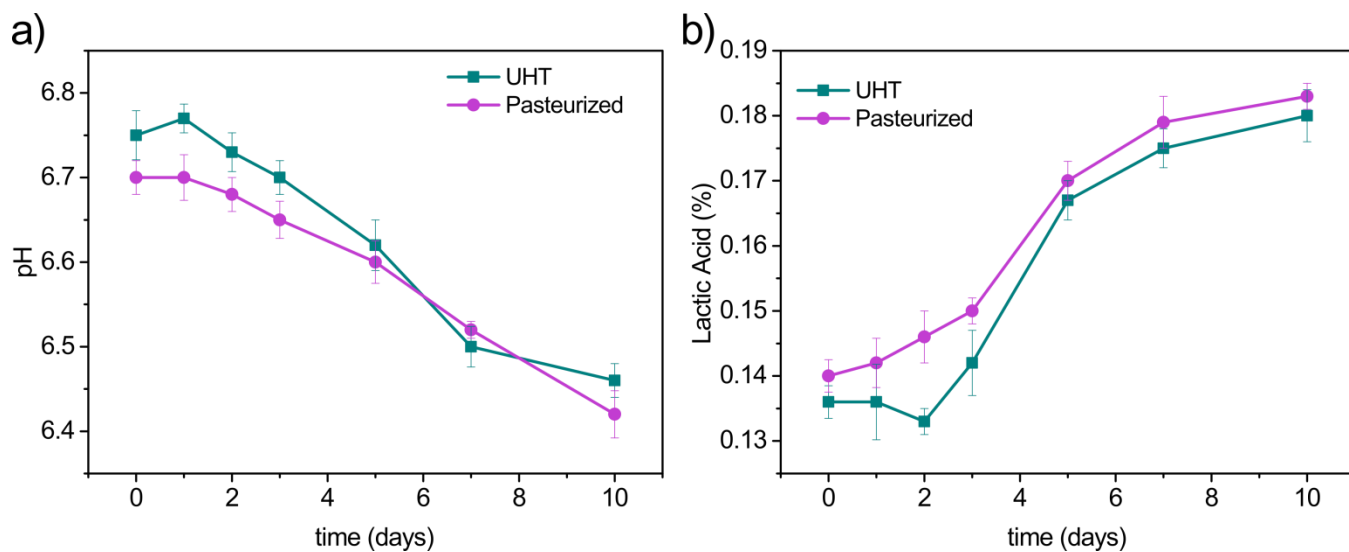


**Figure S8.** Variation of pH (a) and total acidity (b) as a function of time for UHT and pasteurized milk.

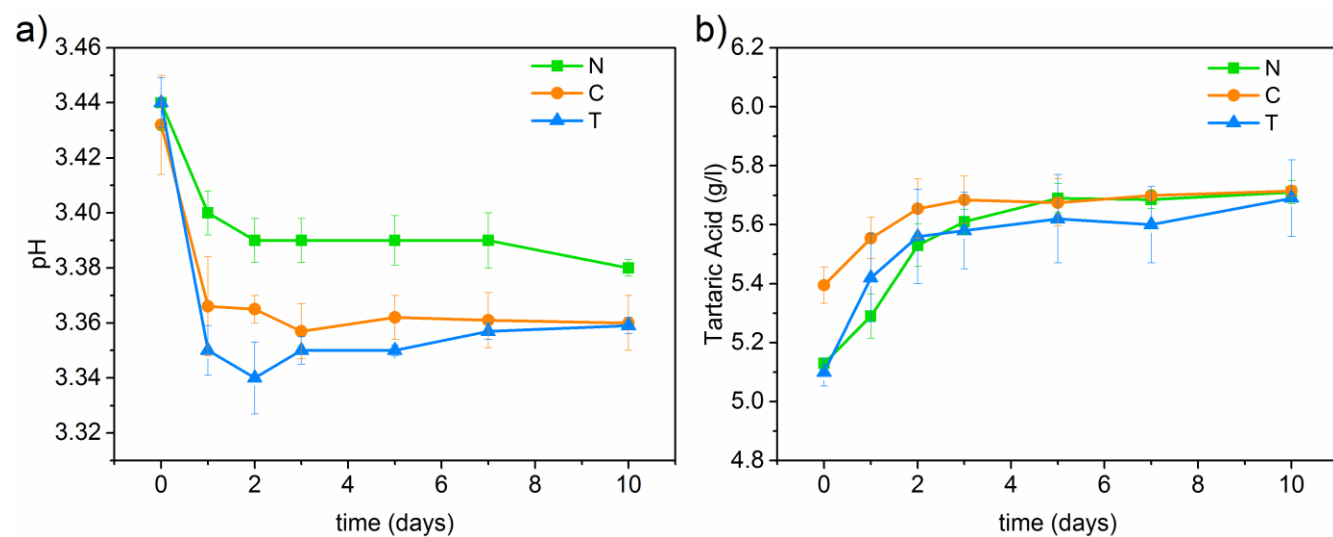


**Figure S9.** Variation of pH (a) and total acidity (b) as a function of time for three different red wines.

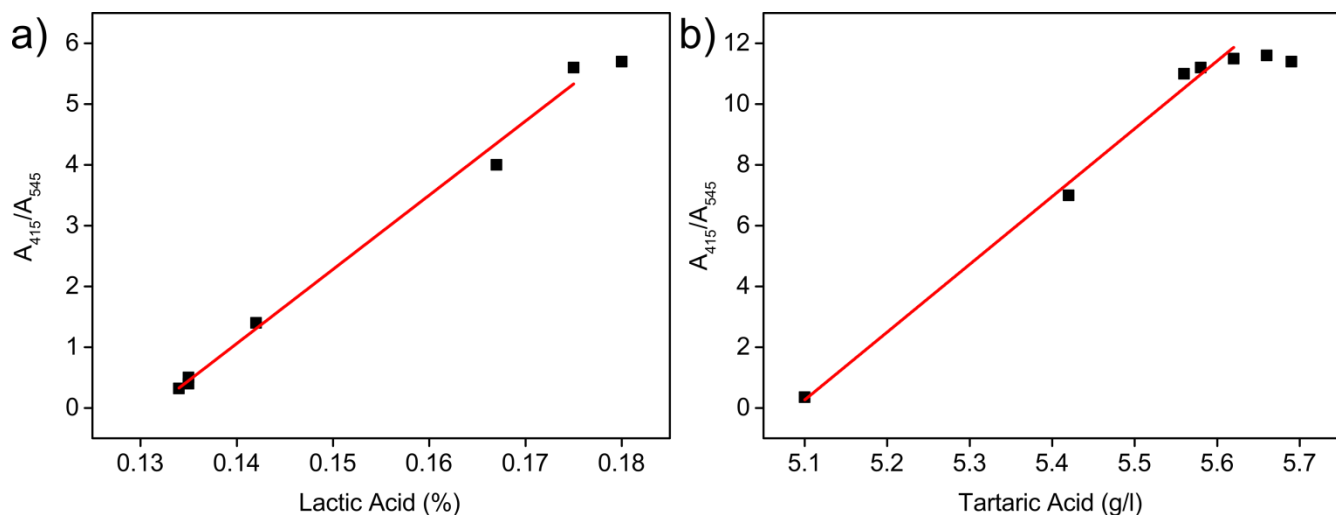


**Figure S10.** Absorbance ratio of MCH (415 nm) and MC (545 nm) as a function of the total acidity of (a) UHT milk and (b) table red wine expressed as lactic acid and tartaric acid respectively.

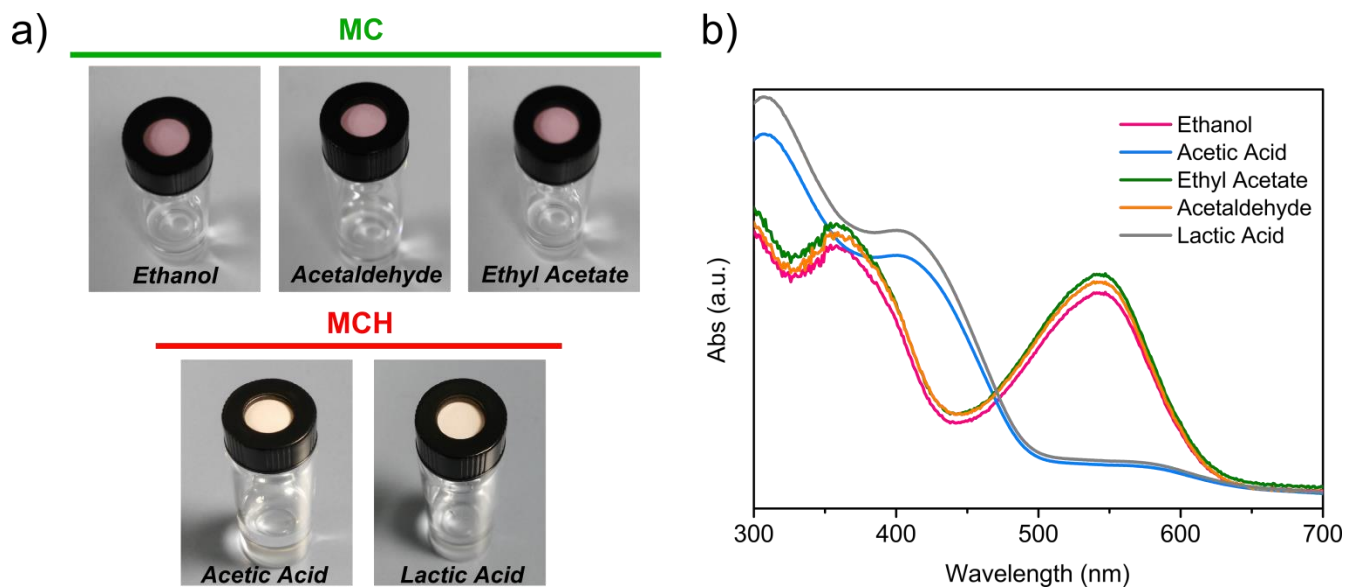


**Figure S11.** Photographs (a) and UV-Vis spectra (b) of UV irradiated FF/SP-PHEMA caps exposed to vapors of ethanol, acetaldehyde, ethyl acetate, acetic and lactic acid for 1h. Similar results were obtained for different exposure times, namely: 60s, 2h, 6h, 24 h, 72h, 5 days, 7 days and 10 days.

## REFERENCES

- (1) Heredia-Guerrero, J. A.; Benítez, J. J.; Cataldi, P.; Paul, U. C.; Contardi, M.; Cingolani, R.; Bayer, I. S.; Heredia, A.; Athanassiou, A. All-Natural Sustainable Packaging Materials Inspired by Plant Cuticles. *Adv. Sustainable Syst.* **2017**, *1*, 1600024.
- (2) Rad, J. K.; Mahdavian, A. R. Preparation of Fast Photoresponsive Cellulose and Kinetic Study of Photoisomerization, *J. Phys. Chem. C* **2016**, *120*, 9985-9991.